Fisheries Research 193 (2017) 195–206

Contents lists available at ScienceDirect

Fisheries Research

journal homepage: www.elsevier.com/locate/fishres

Bomb radiocarbon analyses validate and inform age determination of longnose skate (*Raja rhina*) and big skate (*Beringraja binoculata*) in the north Pacific Ocean

J.R. King[a,*], T. Helser[b], C. Gburski[b], D.A. Ebert[c], G. Cailliet[c], C.R. Kastelle[b]

[a] *Fisheries and Oceans Canada, Pacific Biological Station,3190 Hammond Bay Road, Nanaimo, BC, V9T 6N7, Canada*
[b] *National Oceanic and Atmospheric Administration, National Marine Fisheries Service, Alaska Fisheries Science Center, 7600 Sand Point Way NE, Seattle, WA, 98115, United States*
[c] *Moss Landing Marine Laboratories, Pacific Shark Research Center, 8272 Moss Landing Road, Moss Landing, CA 95039, United States*

ARTICLE INFO

Handled by George A. Rose

Keywords:
Northeast pacific age validation
Bomb radiocarbon
Big skate
Longnose skate

ABSTRACT

Age and growth estimates based on growth band counts of sectioned vertebrae have been produced for longnose skate (*Raja rhina*) and big skate (*Beringraja binoculata* [formerly *Raja binoculata*]) populations in the Gulf of Alaska, British Columbia and California. Previous growth studies involving estimates from different laboratories in the USA (Alaska Fisheries Science Center, AFSC; Pacific Shark Research Center, PSRC at Moss Landing Marine Laboratories) and Canada (Fisheries and Oceans Canada, DFO) have produced dissimilar results for either species, highlighting the need for development of a consistent age determination protocol and more importantly an age validation study. Archived large specimens of longnose skate and big skate collected in Monterey Bay, CA, in 1980 and 1981 had minimum preliminary age estimates from vertebral growth band counts old enough to suggest that radiocarbon (^{14}C) signals from bomb testing conducted in the late-1960s could be used to establish dates of growth band formation. To this end, we micro-milled skate vertebral thin sections, measured $\Delta^{14}C$ using mass spectrometry, and estimated year of growth band formation based on the estimated age from growth band counts using both unstained and stained preparation methods Non-linear random effects modeling, implemented in a Markov Chain Monte Carlo (MCMC) simulation, was used to compare the skate $\Delta^{14}C$ data set to a marine teleost otolith reference chronology for the California Current System. Results showed $\Delta^{14}C$ measurements for big skate were non-informative as none of the archived samples were old enough for comparison to the reference curve, hence validation of the age estimation approach was not possible. However, for longnose skate, $\Delta^{14}C$ data were more informative to fit pulse function models and compare results to the reference chronology. Modeling results indicated longnose skate age estimates based on unstained vertebral thin sections were less biased (overestimated to a smaller degree) than estimates based on stained vertebral thin sections. The degree of bias depended on agency ageing criteria, with the least biased age estimates produced by age readers from the AFSC. The AFSC age estimates had about a 70% probability that age estimates of longnose skate was within +/− 2 years of the expected age based on the radiocarbon assays. We were able to validate the age estimation methodology for longnose skate and establish criteria for growth band counts, which should now be useful to generate region-specific accurate growth and life history parameters required for more reliable stock assessment approaches.

1. Introduction

Along the entire North American west coast, skates are often taken in large numbers as bycatch in groundfish fisheries (Ormseth and Matta, 2009; Haas, 2010; Gertseva, 2009). There is an existing targeted longnose skate (*Raja rhina*) and big skate (*Beringraja binoculata* previously *R. binoculata*) fishery in British Columbia, Canada, with mean annual landings of 1,300 t. A directed fishery for skates emerged in the Gulf of Alaska around Kodiak Island, USA, in 2003, subsequently ended in 2005 (Ormseth and Matta, 2009) and re-emerged in 2010. During 2010, over 14,000 t of skates were taken as bycatch in groundfish fisheries in the Bering Sea and Aleutian Islands, approximately 30% of which were landed. Because of their unique biological traits (e.g. probable long life span, slow growth, low fecundity, and late age at

* Corresponding author.
E-mail address: Jackie.King@dfo-mpo.gc.ca (J.R. King).

http://dx.doi.org/10.1016/j.fishres.2017.04.004
Received 22 September 2016; Received in revised form 10 January 2017; Accepted 10 April 2017

maturity) these species may be at risk of severe population declines that may eventually lead to a compromise in their ability to sustain fishing pressure and recover from overexploitation (Dulvy et al., 2000). Detailed biological information is required for effective management of this vulnerable group. In particular, age determination and age validation, which serve as the most fundamental of data sources for the rationale management of these species, have been largely ignored.

Age estimation for elasmobranchs is limited by the lack of bony structures, but structures such as enameled spines, caudal thorns, vertebrae or haemal arches have been successfully used (see Cailliet and Goldman, 2004 for an extensive review). The current methodology for age estimation for longnose skate and big skate relies on thin sectioning of vertebrae for growth band counts (Zeiner and Wolf, 1993). Age estimates and growth curve estimates have been produced for longnose skate and big skate populations for the Gulf of Alaska (Gburski et al., 2007), British Columbia (Mc Farlane and King, 2006), USA west coast (Thompson, 2006), and central California (Zeiner and Wolf, 1993). However these studies did not produce similar results, but no latitudinal gradient in results was apparent. The differences therefore are likely due to differences among laboratories in interpretation of growth bands, with subsequent differences in estimated ages. It is therefore imperative that age estimation differences between laboratories be reconciled using validated ageing criteria.

In the 1950s and 1960s, the testing of atomic bombs resulted in the rapid increase in atmospheric levels of radiocarbon (^{14}C), which was then subsequently incorporated within the bodies of oceanic organisms (Druffel and Linick, 1978). This period of ^{14}C increase has been used as a date marker in fish structures that exhibit growth bands, such as exemplified in early studies on teleost otoliths (Kalish, 1993) and elasmobranch vertebrae (Campana et al., 2002; McPhie and Campana, 2009). Bomb-produced radiocarbon ^{14}C (Kalish, 1995) however, is only applicable to specimens that were alive during the period of bomb radiocarbon rise. Longnose skate and big skate vertebrae archived in the museum collection at the Pacific Shark Research Center, Moss Landing Marine Laboratories (obtained from the Pacific Shark Research Center, PSRC, Moss Landing, CA) that were collected from commercial bottom trawls in Monterey Bay, CA in 1980 and 1981 (Zeiner and Wolf, 1993), offered the unique opportunity to use bomb radiocarbon analyses for age validation of these two species. These specimens had minimum age estimates of 11–13 years (Zeiner and Wolf, 1993), suggesting that marine radiocarbon signals still present in 1967–1969 from bomb testing could be used to establish dates of growth band formation.

This study was a collaboration among multiple agencies responsible for skate research or management across their population range: California, USA, British Columbia, Canada and Alaska, USA. The goals of this study were to: *i*) compare the $\Delta^{14}C$ pulse function curves for skate radiocarbon data to a $\Delta^{14}C$ reference chronology and estimate the probability of ageing bias; *ii*) investigate the utility of applying a histological stain to vertebral thin sections to enhance band patterns; *iii*) determine which age estimates produced by each agency and which section preparation method were most accurate relative to the $\Delta^{14}C$ chronology, and *iv*) identify the best age determination criteria for counting growth bands based on the later.

2. Materials and methods

2.1. Specimen selection

Longnose skate and big skate vertebrae archived in the museum collection at Moss Landing Marine Laboratories (Moss Landing, CA) were used in this study. These specimens were collected in 1980 and 1981 off the Central California coast near Monterey Bay from commercial catches (Zeiner and Wolf, 1993). The sex and total length (TL, mm) for each specimen was recorded. Information on the specific location of capture (i.e. latitude and longitude), or fishing depth was not available. Only specimens with age estimates (Zeiner and Wolf, 1993) that suggested the fish was alive pre-bomb pulse or during the years of radiocarbon increase (pre-1970) were selected. In total, 33 longnose skate (13 males, 20 females) and 12 big skate (8 males, 4 females) archived vertebrae were used in this study. Total lengths for longnose skate ranged from 68.3 cm to 106.8 cm; and total lengths for big skate ranged from 115.0 to 160.0 cm.

2.2. Age determination

2.2.1. Specimen preparation

For each specimen, a section of the vertebral column (10th–20th centra) was taken, labelled, and frozen. In the laboratory, column sections were thawed; individual centra were separated using a shark knife; the connective tissue and neural arch were removed; and centra were air dried for 24–48 h. Centra were individually embedded in Buehler™ EpoThin© low viscosity epoxy resin using customized silicone wells with a cure time of 9 h. Embedded centra were wet-sectioned along the longitudinal plane using a Isomet™ slow-speed saw and three Buehler™ 3-inch wafering blades (15 HC diamond series) separated by spacers to produce two sections approximately 0.5–0.7 mm thick. Sections were mounted on microscope slides using Crystal Bond™ thermal setting resin and subsequently wet-sanded using successively finer grits of sandpaper (600–1200) followed by 3M™ Wetordry™ polishing paper. Multiple centra per specimen were sectioned and mounted; some for micro-milling and atomic mass spectrometry analyses, others for inter-agency exchange and comparison of vertebrae preparation methods (unstained vs. stained).

For each specimen one vertebral thin section was prepared for age estimation with no stain (unstained preparation method, Zeiner and Wolf, 1993), with mineral oil used at the time of age estimation to enhance band patterns. A second vertebral thin section was prepared for age estimation with a staining technique (stained preparation method) modified from Natanson et al. (2007). This second vertebral thin section was decalcified with a rapid decalcifier, stained with Harris modified hematoxylin, destained with an acid-alcohol solution to remove excess stain, and soaked in glycerin (Natanson et al., 2007).

2.2.2. Ageing criteria

Three agencies took part in age estimation for comparison, each following its own published methodology for estimating annual band pair counts: Alaska Fisheries Science Center (AFSC; Gburski et al., 2007); Fisheries and Oceans Canada (DFO; McFarlane and King, 2006); and PSRC (Zeiner and Wolf, 1993). Common to all methodologies is counting opaque and translucent bands under reflected light as a single annual band pair. However, these band pairs vary in distinctiveness, and are often faint. Therefore, differences remain in the interpretation of these faint zones, some of which may be 'checks' or non-annual band pairs. A check may be due to seasonal changes in growth or may be randomly occurring and should not be counted as an annual mark. Inclusion of checks in annual band pair counts, can overestimate the true age.

2.2.3. Inter-agency comparison of age estimations and ageing precision

The longnose skate and big skate vertebrae thin sections were exchanged between agencies, with each agency providing two readers who estimated the number of band pairs independently of one another. Each reader estimated the number of bands pairs. Intra-agency (between-reader) precision was calculated by using the coefficient of variation (CV; Chang, 1982), percent agreement between readers (Goldman, 2004) and average percent error index (APE; Beamish and Fournier, 1981). Campana (2001) suggested that acceptable levels of mean CV and APE would be less than 7.6% and 5.5%, respectively. Intra-agency systematic bias was assessed with pairwise age-bias plots (Campana et al., 1995) and the Evans-Hoenig chi-squared test of symmetry (McBride, 2015).

2.3. Age validation

2.3.1. Specimen micro-milling

The accuracy of using vertebral growth band counts to estimate age was assessed using bomb radiocarbon analyses provided by atomic mass spectrometry (AMS). To obtain sufficient material for ^{14}C analyses, multiple vertebral thin sections per skate specimen were milled with a high-resolution micro-milling system (Carpenter Systems™ CM-2). Due to the small size of the vertebrae, multiple whole pieces corresponding to the same growth bands, but from different corpus calcarea, were extracted and pooled for a minimum of 5 mg per sample. Sampling regions of specific growth bands were pre-selected from digital images produced using a Leica™ MZ75 microscope with attached Leica™ DFC320 R2 digital camera and associated Leica™ Application Suite 3.1.0 software. The images were adjusted with Adobe™ Photoshop 1.12 to enhance the contrast between adjacent growth bands and to increase overall sharpness and clarity. Growth band pairs (opaque and translucent growth bands viewed under reflected light) were considered to be a single annual band pair. The first 1–3 annual band pairs (i.e. those near the focus: inner growth zones), and the final 1–3 annual band pairs (i.e. those near, but excluding, the margin: outer growth zones) were milled carefully to ensure no resin contamination. The mid-point estimate of year of deposition for these samples of 1–3 band pairs was used as the sample year of deposition.

2.3.2. Radiocarbon assays

The micro-milled samples were sonicated in Super Q water, dried and then weighed to the nearest 0.1 mg. Assays of ^{14}C for extracted growth zones were completed via AMS by Beta Analytic Inc., Miami, Florida, USA (ISO/IEC 17025:2005 accredited). AMS also provided $\delta^{13}C$ (‰) values used to correct for any isotopic fractionation variation and determine the source of carbon. Following to the methods of Stuvier and Polach (1977), radiocarbon values were subsequently reported as $\Delta^{14}C$, which is the per mil (‰) deviation of the sample from the radiocarbon concentration of 19th century wood, corrected for sample decay normalized to 1950. The mean standard deviation calculated from the percent modern carbon of the individual radiocarbon assays was < 4‰.

2.3.3. Statistical modeling

The approach for age validation based on bomb radiocarbon analysis is to mathematically compare the validation sample $\Delta^{14}C$ estimates (skates) to a reference carbonate chronology, here to petrale sole (*Eopsetta jordani*) otoliths (Haltuch et al., 2013), which is considered an appropriate reference for the California Current System (Helser et al., 2014). The validation sample consisted of ages estimated by each reader based on growth zone counts of unstained and stained vertebrae. The modeling of ^{14}C incorporation can be described as a 4-parameter logistic (4PL) model (Appendix C.6 in Pinheiro and Bates, 2000) with a trivial modification. The 4PL model relates the dependent variable, $\Delta^{14}C$, to the deposition year (denoted by t) by the i^{th} age reader for the j^{th} fish specimen via a sigmoidal function, expressed by:

$$y_{ij} = \theta_1 + \frac{\theta_2}{1 + \exp[((\theta_3 - u_{i3}) - t_{ij})/(\theta_4 + u_{i4})]} + e_{ij} \quad (1)$$

Where: θ_1 is the lower horizontal asymptote as $t \rightarrow -\infty$; θ_2 is the total increase of $\Delta^{14}C$ from θ_1; θ_3 is the t-value at inflection point or the deposition year at 50% of θ_2; $\theta_4 > 0$ is a scale parameter on the x-axis.

The upper horizontal asymptotic as $t \rightarrow \infty$ is calculated by $\theta_1 + \theta_2$. When $t = \theta_3 + \theta_4$ the response, $y = \theta_1 + (\theta_2)/(1 + e^{-1})$, is roughly three-quarters of the distance from θ_1 to the upper asymptote, $\theta_1 + \theta_2$ (Appendix C.6 in Pinheiro and Bates, 2000). We assume that the random error of the model is normally distributed $e_{ij} \sim N(0, \sigma_e^2)$. In our approach to estimation, we used a non-linear mixed effects model by treating ages generated by each independent age reader (including the petrale sole reference data set) as a random effect. This treats the nested nature of the data simultaneously and accounts for their overall mean structure as well as their variability both within and between subjects (age readers). As such, we are interested in estimating both the fixed-effect model parameters, $\theta = (\theta_2, \theta_3, \theta_4)'$, two random-effect parameters, $\boldsymbol{u} = (u_{i3}, u_{i4})$, and four variance components. The full variance-covariance structure of the model is

$$V = \begin{bmatrix} G & 0 \\ 0 & R \end{bmatrix}, \text{ where } \mathbf{G} \sim MVN(\theta, \Sigma) \text{ and } \Sigma = \begin{bmatrix} \sigma^2_{\theta 3} & \sigma^2_{\theta 34} \\ \sigma^2_{\theta 43} & \sigma^2_{\theta 4} \end{bmatrix}$$ is the random effect variance component assumed to be independent realizations from a multivariate normal distribution with mean zero and 2×2 unstructured covariance matrix. The model error variance is $R_i(\theta) = \sigma^2 I_{t_i}$, where I_{t_i} is the $t_i x t_i$ identity matrix and the variance-covariance matrix depending on the vector of unknown parameters $\boldsymbol{\theta}$.

To fit the data we fixed the parameter for the lower asymptote, θ_1, to the lowest value (-110‰) in the combined data sets (skates and petrale sole) as suggested by Hamel et al. (2008). This was due to the difficulty estimating it freely given high parameter correlation and lack of observations for skates at the pre-bomb level. The parameters, θ_1, θ_2, can largely be treated as nuisance parameters because they represent total atmospheric input of $\Delta^{14}C$ concentration into the marine environment at different times, and not rates of increase. Moreover, a principal assumption for using a reference data set, such as petrale sole, is that both the validation (skate) sample and the reference (petrale sole) data are subjected to equivalent marine environmental conditions and biological processes affecting the assimilation of ^{14}C into the structures. As such, the remaining parameters, θ_3, θ_4, are of specific interest as they measure either the timing of increase after the onset of nuclear testing or mis-assignment of age leading to ageing errors and hence differences (or shifts) between the validation and reference curves. In this case, we are estimating these parameters simultaneously by treating them as random effects with the goal to compare the offset between the validation specimen ($i = 1, 2, 3, 4, 5, 6$ readers) and reference chronology, $\Delta(\theta_{i3} - \theta_{R3})$, as a measure of ageing bias.

Markov Chain Monte Carlo (MCMC) simulation was employed to construct a distribution that provides a probabilistic means of quantifying ageing bias, if it exists. Specific mathematical details of this approach including specification of model structure, parameters, priors and implementation in WinBUGS [Bayesian inference Using Gibbs Sampling, (Lunn et al., 2000)] can be found elsewhere (Helser et al., 2014; Kastelle et al., 2015) and are not reiterated here. In general, we specified non-informative conjugate priors to ensure that the likelihood dominated the prior as suggested by Smith and Wakefield (1994). The prior for the variance-covariance matrix **G** was specified by an inverted Wishart distribution (Von Rosen, 1997), with a precision parameter of 10 and mean matrix $0.1 \times \mathbf{I}$. Priors for fixed model parameters were specified as multivariate normal distributions with zero mean and covariance matrix with diagonal elements equal to 1000, and off-diagonal elements equal to zero. Forσ_e^2, Spiegelhalter et al. (2003) recommend a default inverse-gamma prior for σ_e^{-2} in WinBUGS, i.e., σ_e^{-2}~dgamma (0.001, 0.001).

The estimated parameters were evaluated based on 2000 samples (first half of a 1,000.000 draw chain was discarded) thinned at a rate of every 250th sample from MCMC simulation of the joint posterior distribution. Bayesian diagnostic procedures were performed to evaluate convergence of the MCMC simulation to the target posterior distribution and model goodness of fit to the data as prescribed in Gelman et al. (2004). Evidence for age determination bias (+/−) based on the validation sample (for any given age reader i) and reference curve (R) can be calculated as the tail probability greater or less than zero; e.g., Prob$[\Delta(\boldsymbol{\theta}_{i3} - \boldsymbol{\theta}_{R3})] > 0$.

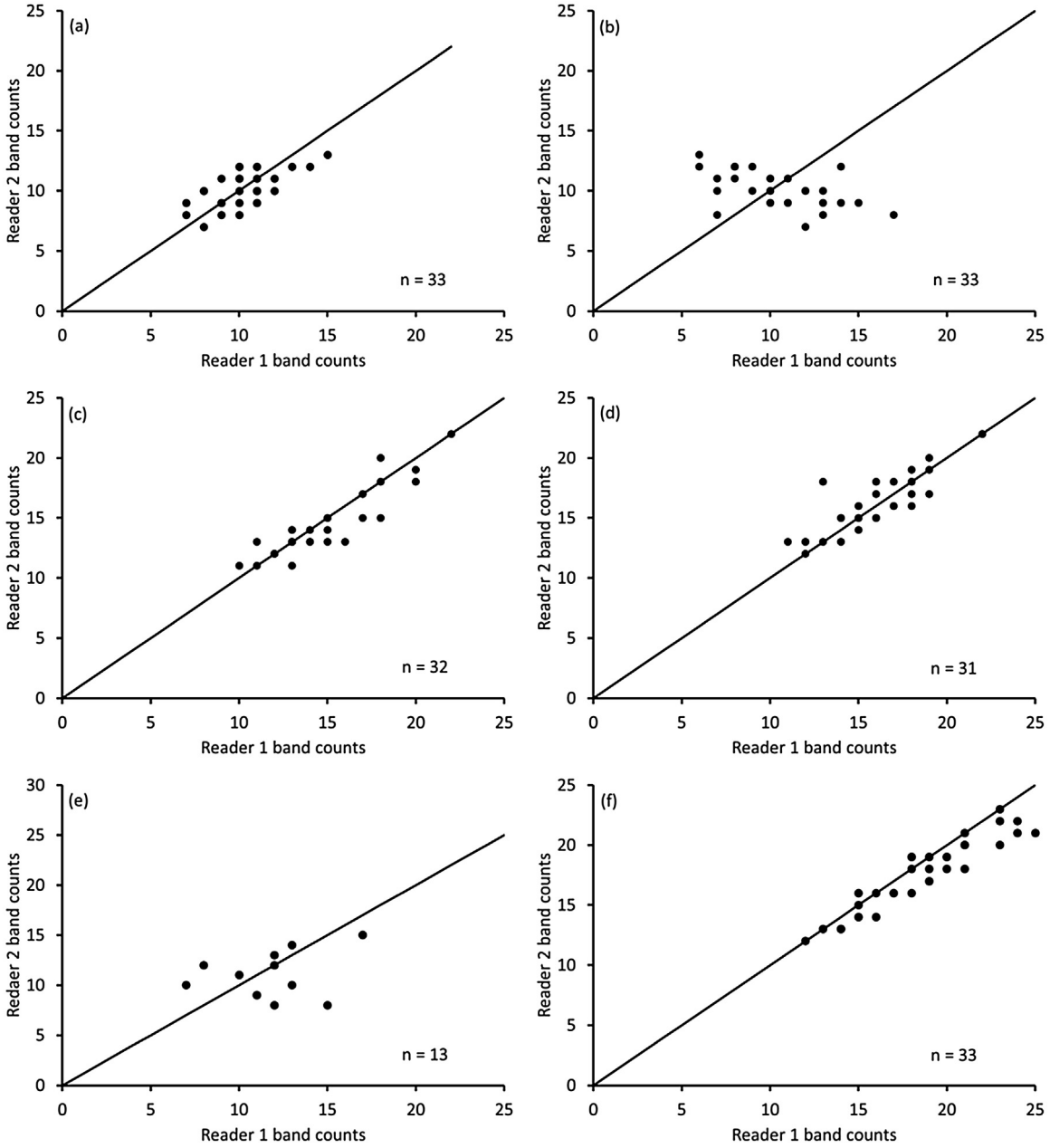

Fig. 1. Longnose skate (*Raja rhina*, sexes combined) inter-reader age bias plots for unstained (left column) and stained (right column) thin sections. Reader 1 estimated age (years) vs reader 2 estimated age (years) for Alaska Fisheries Science Center (AFSC) (a) and (b); Fisheries and Oceans Canada (DFO) (c) and (d); Pacific Shark Research Center (PSRC) (e) and (f). The diagonal line represents the one to one equivalence line.

3. Results

3.1. Age estimates and precision

3.1.1. Longnose skate

The lowest age estimates for longnose skate were produced by the AFSC, ranging from 7 to 17 years (Fig. 1). The age estimates by one of the AFSC readers were lower for the stained preparation method than for the unstained preparation method (Fig. 1). The age estimates produced by DFO ranged from 10 to 22 years, with no difference in age estimates between preparation methods (Fig. 1). The DFO could not assign ages for a few of the samples (n = 1 unstained; n = 2 stained). The PSRC could assign ages for most (n = 20) of the unstained samples. The ages estimated by the PSRC for stained samples ranged from 7 to 25 years; this age range was higher than those the PSRC estimated for the unstained samples (Fig. 1).

The intra-agency percent agreement (± 0 years) for longnose skate ages never exceeded 53%, however the AFSC readers for the unstained preparation method reach 100% agreement at ± 2 years (Table 1). The mean CV and APE for DFO readers indicated an acceptable level of precision between readers for either preparation method and an acceptable level for the stained preparation method only between the PSRC readers (Table 1). The inter-reader age bias plots for longnose skate indicated progressive bias between readers at the AFSC for the stained preparation method (Fig. 1), and mean CV and APE for both preparation methods were below acceptable levels (Table 1). Chi-squared tests of symmetry indicated bias between readers at the AFSC for the stained preparation method (McNemar's: $\chi^2 = 18.615$, df = 1, $p < 0.001$; Evans-Hoenig: $\chi^2 = 19.600$, df = 7, $p = 0.007$; Bowker: $\chi^2 = 21.200$, df = 17, $p = 0.218$). The PSRC inter-reader age bias plots for the both preparation methods indicated that one reader produced higher band counts for younger fish and lower band counts for older

Table 1
Longnose skate (*Raja rhina*) and big skate (*Beringraja binoculata*) inter-reader age estimate precision as measured by percent agreement, coefficient of variation (CV) and average percent error index (APE) by agency (Alaska Fisheries Science Center, AFSC; Fisheries and Oceans Canada, DFO; Pacific Shark Research Center, PSRC) and preparation method, sexes combined.

Agency	Preparation	*n*	Percent Agreement			CV	APE
			± 0 years	± 1 years	± 2 years		
Longnose skate							
AFSC	Unstained	33	15.2	63.6	100.0	8.47	5.99
AFSC	Stained	33	21.2	51.5	60.6	14.38	10.17
DFO	Unstained	32	53.1	75.0	93.8	3.78	2.68
DFO	Stained	31	29.0	83.9	96.8	4.42	3.12
PSRC	Unstained	13	15.4	38.5	61.5	15.21	10.76
PSRC	Stained	33	27.3	69.7	87.9	4.45	3.14
Big skate							
AFSC	Unstained	12	0.0	33.3	41.7	20.17	14.26
AFSC	Stained	12	16.7	41.7	75.0	14.02	9.91
DFO	Unstained	12	50.0	66.7	75.0	4.99	3.53
DFO	Stained	12	41.7	58.3	75.0	5.82	4.12
PSRC	Unstained	12	8.3	16.7	33.3	21.38	15.12
PSRC	Stained	12	8.3	41.7	75.0	10.15	7.18

fish (Fig. 1). However, chi-squared tests of symmetry indicated bias between PSRC readers only for the stained preparation method (McNemar's: $\chi^2 = 13.500$, df = 1, $p < 0.001$; Evans-Hoenig: $\chi^2 = 14.571$, df = 4, $p = 0.006$; Bowker: $\chi^2 = 21.333$, df = 17, $p = 0.212$).

3.1.2. Big skate

For big skate, agency age estimates varied greatly with the oldest age estimates produced by DFO and the youngest produced by the AFSC (Fig. 2). The intra-agency percent agreement (± 0 years) was typically low, ranging from 0% for AFSC readers on the unstained preparation method to 50% for DFO readers and the unstained preparation samples (Table 1). Intra-agency percent agreement at ± 2 years, reached 75% for the stained preparation samples (Table 1). The mean CV and APE for the DFO readers indicated an acceptable level of precision (Table 1). The intra-agency age bias plots for big skate indicated systematic bias between readers at the AFSC for both preparation methods, and a mixed bias between readers at the PSRC for the unstained preparation method where one reader produced higher band counts for younger fish and lower band counts for older fish (Fig. 2). However, chi-squared tests of symmetry indicated bias only between readers at the AFSC for the unstained preparation method (McNemar's: $\chi^2 = 5.333$, df = 1, $p = 0.021$; Evans-Hoenig: $\chi^2 = 8.000$, df = 6, $p = 0.238$; Bowker: $\chi^2 = 12.000$, df = 11, $p = 0.363$).

3.2. Age validation

3.2.1. Radiocarbon analyses

The $\delta^{13}C$ values for both longnose skate (mean = −16.96‰, SE = 0.79) and big skate (mean = −13.08‰, SE = 0.28) (Table 2) indicated a dietary source of carbon rather than dissolved inorganic carbon (DIC, Fry, 1988). Many of the samples of longnose skate did not have $\delta^{13}C$ values since the amount of material was large enough only for ^{14}C assays. For longnose skate, the $\Delta^{14}C$ values generally increased from the inner growth zones (earlier years) to outer growth zones (later years) (Table 2). Based on Haltuch et al. (2013), $\Delta^{14}C$ values for inner growth zones were expected to be negative, between −80 and −120‰, if they were deposited in the pre-bomb signal period (pre-1959) and to rapidly become positive if they were deposited in the increase period (1965-70). None of the longnose skate samples had $\Delta^{14}C$ values for the inner growth zones that were between −80‰ and −120‰ (Table 2). However, 10 longnose skate samples had $\Delta^{14}C$ values for the inner growth zones that were between −80‰ and 0‰ (Table 2). None of the $\Delta^{14}C$ values for big skate inner growth zones were negative, with the exception of sample RB6 (Table 2).

3.2.2. Statistical modeling

3.2.2.1. Longnose skate. Based on $\Delta^{14}C$ measurements and the associated year of deposition from ageing estimates, pre-1962 data were unavailable (Fig. 3). The earliest values of longnose skate $\Delta^{14}C$ measurements occurred in 1963 and thus the lack of observations during the pre-bomb and initial rise created difficulties of estimating the lower asymptote of the pulse function. Most of the longnose skate $\Delta^{14}C$ measurements during the years 1963–1970, generally are above the petrale sole reference values. The number of parameters estimated was dependent on the preparation method, (stained vs. unstained) because the PSRC could not assign ages for most of the unstained preparation method specimens. Hence, both methods resulted in the estimation of three fixed parameters and three variance components, but 10 and 14 random effect parameters were estimated for the unstained and stained preparation methods respectively. Examination of model results between the two preparation methods was only possible between the AFSC and DFO and while the results did not show substantially different pulse functions it should be noted that the random effects variance ($\sigma_r^2 = 58.13$) was 3 times as large for the stained preparation method suggesting greater between reader variability in age estimates (Fig. 4, lower panel). As such, our analysis and reported results focused on the unstained preparation method (Table 3; Fig. 4, upper panel).

The MCMC simulation outputs and diagnostics for the resultant non-linear mixed effects model fits to the longnose skate and petrale sole reference data suggested efficient sampling, and evidence of convergence to a stationary posterior distribution (Table 3, Fig. 5). Trace and kernel density plots of the posterior sample ($n = 2000$) indicated the MCMC simulation traversed the parameter space efficiently (Fig. 5) and convergence diagnostics of thinned chain sequence 1st order correlation and Geweke statistics further supported evidence of convergence (Table 3). As such, the posterior sample of parameters and derived quantities were used to compare longnose skate and petrale sole pulse functions and quantify ageing bias.

The comparison of the reader and agency-specific pulse curves to the petrale sole reference curve identified discrepancies between agency age estimates (Fig. 4). The age estimates based on the unstained preparation method provided by AFSC age readers resulted in the best coherence to the petrale sole reference curve. In general, AFSC age reader curves were somewhat left-shifted by about 1–3 years while DFO age reader curves were left-shifted by about 6–7 years. The PSRC age readers could not provide age estimates for the unstained preparation method. For the stained preparation method, the same general pattern was also observed except that in this instance the PSRC age readers did provide age estimates which were left-shifted by as much as 10–12 years (Fig. 4). In general, these results suggest that all three agencies

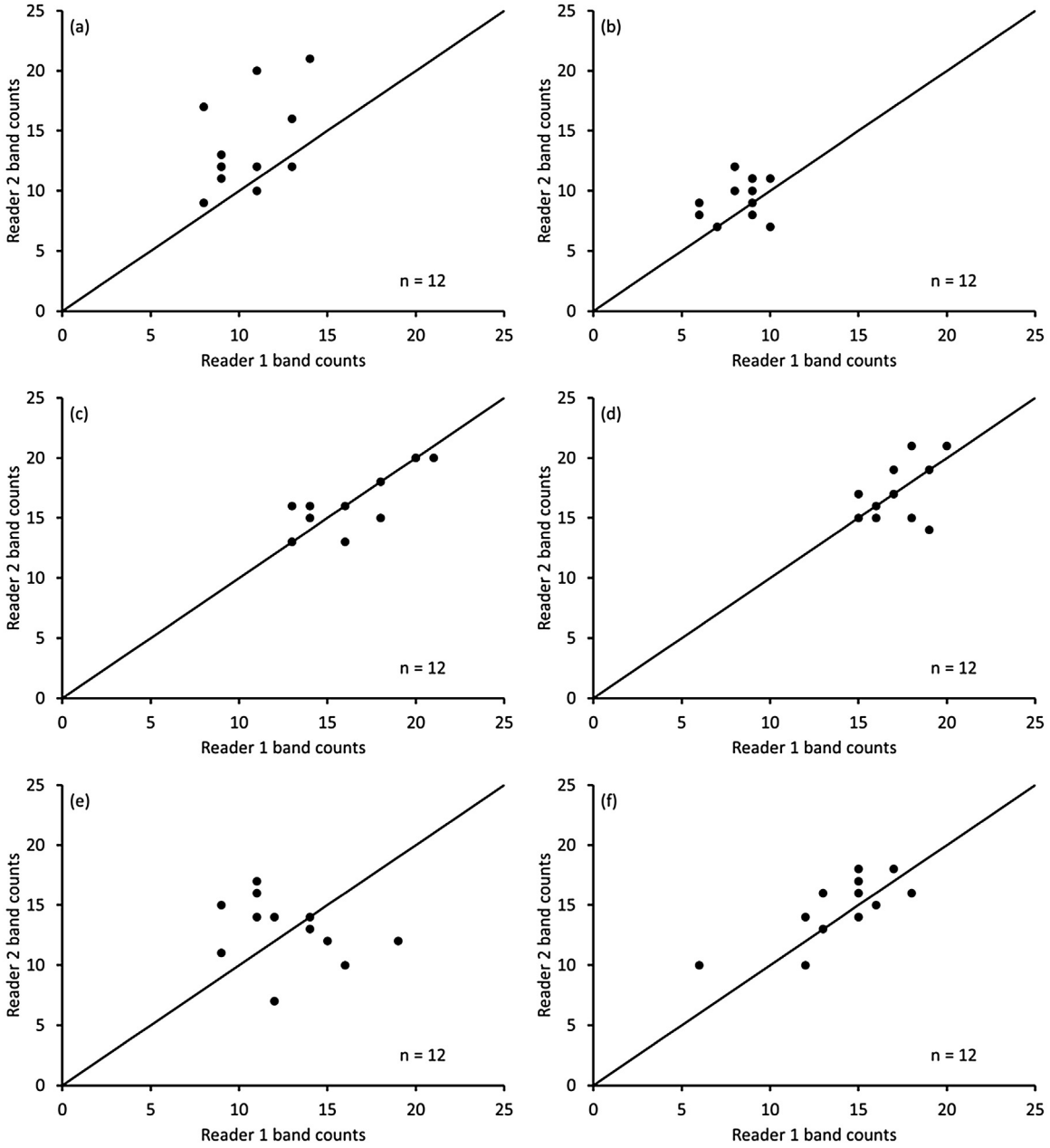

Fig. 2. Big skate (*Beringyraja binoculata*, sexes combined) inter-reader age bias plots for unstained (left column) and stained (right column) thin sections. Reader 1 estimated age (years) vs. reader 2 estimated age (years) for AFSC (a) and (b); DFO (c) and (d); PSRC (e) and (f). The diagonal line represents the one to one equivalence line.

overestimated longnose skate ages to varying degrees, but that AFSC interpretation of the annual band pairs was the least biased (i.e. overestimation of age).

Ageing bias based on unstained sections was quantified as $\Delta(\theta_{i3} - \theta_{R3})$ by using the posterior sample for each age reader within the AFSC and DFO (Fig. 6). Posterior densities of AFSC ageing bias was quite similar between the two readers showing the highest posterior density of overestimation by about 2 years (negative values indicate overestimation). Approximately 5% to 10% of the posterior density encompassed zero, so accurate age estimates can be rendered assuming the petrale sole $\Delta^{14}C$ data approximates a valid assay. For DFO interpretation of the same specimens, the two age readers were consistent with each other, but both overestimated longnose skate ages by about 7 years (highest posterior density). Neither DFO reader had posterior densities encompassing zero ageing bias, suggesting an unequivocal over-counting of annual band pairs which would very rarely result in an accurate longnose skate age estimate from a random sample of vertebrae.

3.2.3. Big skate

Since the $\Delta^{14}C$ values for big skate appeared to represent a post-bomb signal period only (Fig. 3), no modeling was done for these samples. Without $\Delta^{14}C$ values relating to the pre-bomb or rapid signal increase periods, any amount of bias (if present) cannot be estimated. The age determination methodology for big skate cannot be validated with bomb radiocarbon analyses of these samples.

4. Discussion

The radiocarbon results for the archived big skate samples indicated that the specimens were not alive during the pre-bomb signal period, or during the rapid signal period. As such, the age determination methodology for big skate cannot be validated with bomb radiocarbon analyses of these samples. Longnose skate bomb radiocarbon samples

Table 2
Sample summary and the $\delta^{13}C$ (‰) and $\Delta^{14}C$ (‰) assay results for inner growth zones (first 1–3 bands) and outer growth zones (last 1–3 bands) extracted from longnose skate and big skate vertebrae used for bomb radiocarbon analyses.Table 1 *continued.*

Species	Sample	Total length (cm)	Sex	Year collected	Inner growth zones		Outer growth zones	
					$\delta^{13}C$	$\Delta^{14}C$	$\delta^{13}C$	$\Delta^{14}C$
Longnose skate	RR1	1060	2	1981	-13.3	-46.37	-15	27.25
	RR2	1068	2	1981	-12.3	-31.65	–	-2.41
	RR3	972	2	1980	-12.3	-18.79	–	39.24
	RR4	840	1	1981	–	40.11	-15.3	50.98
	RR5	952	1	1981	–	27.25	–	57.9
	RR6	872	2	1981	–	29.23	-15.4	47.03
	RR7	920	2	1981	–	23.3	–	65.81
	RR8	856	1	1981	–	20.33	-20.1	61.86
	RR9	820	1	1981	–	7.48	–	34.17
	RR10	941	1	1981	–	-41.96	–	31.21
	RR11	930	2	1981	–	43.07	–	49.99
	RR12	895	1	1981	–	34.17	–	48.02
	RR13	800	2	1981	–	-31.08	-14.8	8.47
	RR14	800	1	1981	–	-25.15	–	34.17
	RR15	980	1	1981	–	36.15	–	36.15
	RR16	736	1	1981	–	26.26	–	42.08
	RR17	930	1	1981	–	-53.82	–	26.26
	RR18	893	1	1981	–	-1.42	–	43.07
	RR19	919	1	1981	–	11.43	–	26.26
	RR20	951	2	1981	–	-11.31	–	23.3
	RR21	950	2	1981	–	8.47	-14.5	20.33
	RR22	880	2	1981	–	38.13	–	36.15
	RR23	918	2	1981	–	25.28	–	46.04
	RR24	860	2	1980	–	18.48	-16.9	39.24
	RR25	854	2	1980	–	38.25	-15.1	36.28
	RR26	870	2	1980	-19.7	-25.03	–	6.61
	RR27	893	2	1980	–	44.19	–	46.17
	RR28	890	2	1980	-17.4	39.24	–	52.1
	RR29	946	2	1980	–	-55.68	-19.7	55.06
	RR30	870	2	1980	-23.7	39.24	-19.9	36.28
	RR31	855	2	1980	–	26.39	-19.3	58.03
	RR32	845	2	1980	–	30.34	–	50.12
	RR33	683	1	1981	–	38.13	–	43.07
Big skate	RB1	1600	2	1981	-12.9	31.95	-11.9	37.23
	RB2	1235	1	1981	-10.9	7.95	-12.4	5.7
	RB3	1230	2	1981	-11.7	22.61	-11.5	38.91
	RB4	1370	2	1980	-14.1	68.15	-11.4	45.65
	RB5	1190	2	1981	-13.7	58.76	-11.5	25.8
	RB6	1311	1	1981	-15.3	-52.76	-12.6	66.83
	RB7	1310	1	1981	-15.3	26.82	–	38.13
	RB8	1460	1	1980	-12.5	30.66	–	39.24
	RB9	1220	1	1981	-14	68.56	-13.7	64.44
	RB10	1170	1	1980	-13.7	46.05	-14.3	58.62
	RB11	1150	1	1981	-15.2	49.83	-12.4	55.86
	RB12	1320	1	1981	-13.9	60.34	-12.8	69.76

and associated deposition year data, while limited in the pre-bomb and initial rise era, were nonetheless useful to compare to the petrale sole reference chronology. It is important to note, that for both species we needed to combine material from the first 1–3 annual band pairs in order to obtain sufficient quantity for radiocarbon assays. This might have limited our ability to detect pre-bomb or initial rise era levels of radiocarbon. However, the impact is likely negligible since the year of deposition assigned to each sample was the mid-point estimate of the three annual bands. Inter-agency differences in age estimates of longnose skate exist to varying degrees, but comparison of agency-specific estimated year of deposition and radiocarbon values to the reference chronology identified the most appropriate methodology of assigning annual counts to vertebrae band pairs. Based on the modeling results, the unstained preparation method for thin sections, using the ageing criteria of Gburski et al. (2007), produced the least between reader variability (100% agreement for ± 2 years) and the most accurate age estimates.

The longnose skate age estimation criteria outlined in Gburski et al. (2007) includes a band pair counted as an annulus only if it is consistent across the whole thin section, i.e., the band pair appears on one corpus calcareum 'arm', runs across the intermedialia, and appears on the opposite corpus calcareum. Difficulties in applying this criterion might occur when wet sanding of the mounted thin section unevenly wears the corpus calcareum, so care must be taken at this stage of thin section preparation. Additionally, longnose skate vertebral thin sections have a deeply concave intermedialia, making it difficult to follow outer band pairs across the intermedialia (Fig. 7). An approach to deal with this obstacle, is to 1-where the intermedialia is present, count band pairs only if they are observed from one corpus calcareum, across the intermedialia to the other and; 2-where the intermedialia is not present, compare the banding patterns (i.e. variations in band widths) on the two opposing corpus calcareum and include a band pair in the annual count only if it is evident in the banding pattern of both corpus calcareum (Fig. 7). An eyepiece micrometer can aid in keeping track of potential band pairs by their distance from the focus of the thin section.

The longnose skate radiocarbon pulse curve from AFSC age estimates was most synchronous among the agencies participating in this study with the petrale sole reference curve from the same region.

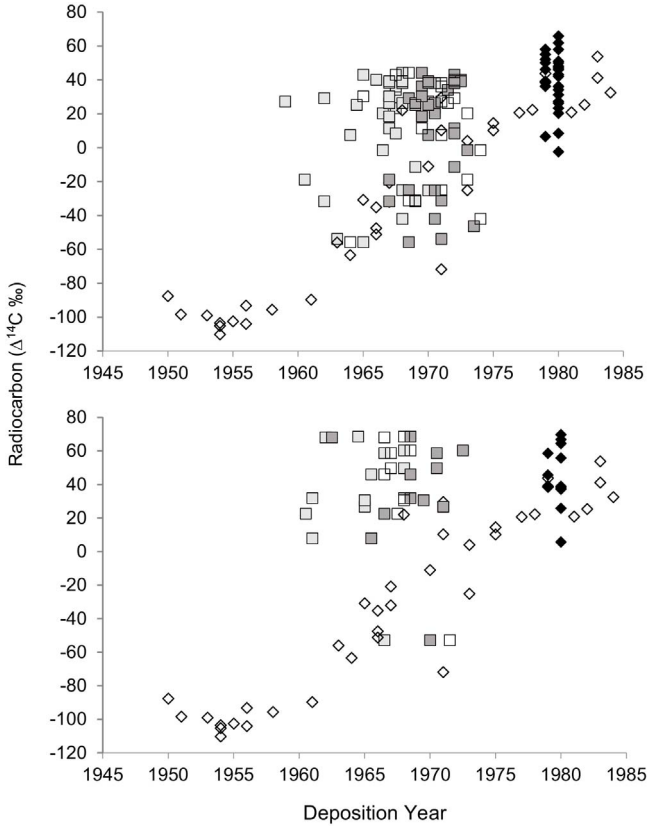

Fig. 3. Petrale sole (*Eopsetta jordani*) radiocarbon [Δ^{14}C (‰)] reference data (open diamonds) and longnose skate (upper panel) and big skate (lower panel) validation radiocarbon [Δ^{14}C (‰)] data (also shown in Table 2). For inner growth zones, the deposition year is based on mean estimated ages by AFSC (dark gray squares), DFO (light gray squares) and PSRC (open squares) age readers for unstained samples. For outer growth zones (solid diamonds), the deposition year is based on year the specimen was collected.

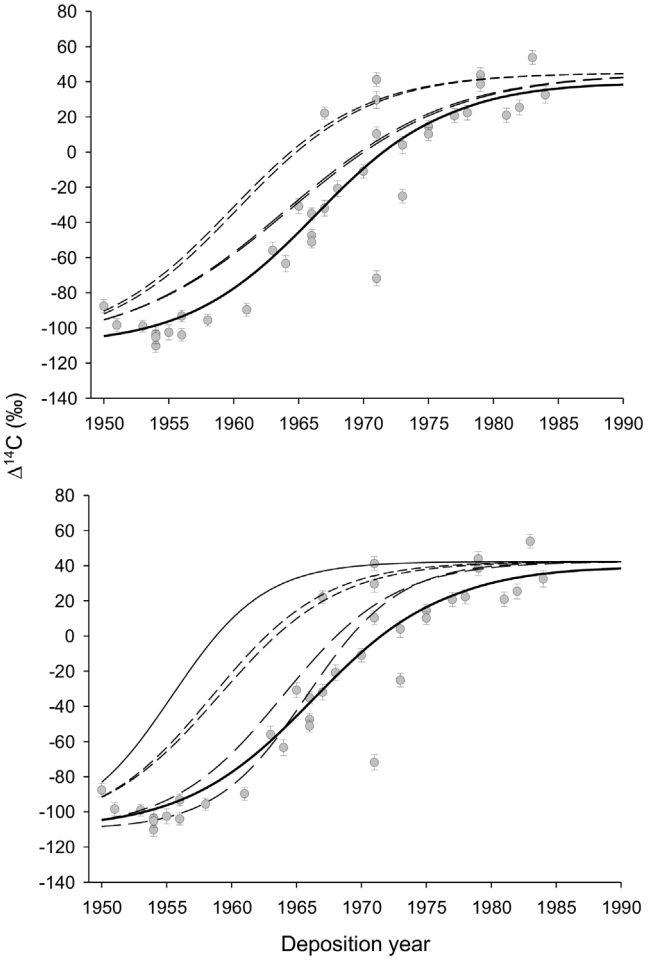

Fig. 4. The agency-specific longnose skate radiocarbon (Δ^{14}C [‰]) pulse curves (for unstained preparation method (top) and stained preparation method (bottom)) produced from each independent age reader compared to the petrale sole reference radiocarbon pulse curve (thick solid line and circles). Long-dashed lines: AFSC age readers; short-dashed lines: DFO age readers; thin-solid lines; PSRC age readers.

Synchrony to a reference curve has been observed in sand tiger shark (*Carcharias taurus*) (Passerotti et al., 2014); however, for other elasmobranch apex predators a phase lag of up to 3–15 years in the rapid rise of Δ^{14}C has been observed when compared to reference chronologies with the resultant elasmobranch pulse curve shifted right (Campana et al., 2002; Ardizonne et al., 2006; Kerr et al., 2006; Passerotti et al., 2010; Andrews and Kerr, 2015). We did not have any young specimens collected during the Δ^{14}C rise period to provide known age material to allow us to identify if the longnose skate radiocarbon pulse should be synchronous or phase lagged to the petrale sole reference chronology. Kerr et al. (2006) identified three possible sources of the delay in rapid rise of Δ^{14}C in elasmobranch vertebrae: 1) metabolic reworking of vertebral collagen, 2) depleted dietary sources of carbon, and 3) age underestimation. However, Kerr et al. (2006) rejected reworking of the vertebrae as an explanation for the phase lag since isotope values were preserved across longitudinal sections of the vertebrae irrespective of differences in Δ^{14}C. This supported assessments based on consistency of within shark Δ^{14}C values made by Campana et al. (2002) and by Ardizonne et al. (2006) that metabolic reworking of elasmobranch vertebrae is minimal and that carbon in the vertebral material is metabolically and temporally stable. Age underestimation was ruled out by Campana et al. (2002) and Kerr et al. (2006) since those studies were able to use young samples collected during the Δ^{14}C rise period which served as known age material. Generally, phase lags in radiocarbon signals in elasmobranchs have been attributed to a dietary source of carbon because any carbon incorporated in the vertebrae from a prey signature is older than the surrounding water (Campana et al., 2002; Kerr et al., 2006; Ardizonne et al., 2006). This phase lag is more evident in apex predators since radiocarbon is carried through more trophic levels (Ardizonne et al., 2006).

The δ^{13}C levels from bomb radiocarbon analyses of longnose skate vertebrae indicated a dietary uptake of carbon rather than DIC (Fry, 1988; 1995; Kalish and Johnston, 1995). Longnose skate are generalist feeders, with an ontogenetic shift in dietary preference at a size of about 60 cm TL from primarily crustaceans and cephalopods to primarily teleosts (Robinson et al., 2007). This shift reflects gape width limitations and weaker foraging ability in smaller skates (Robinson et al., 2007). However, longnose skate inhabiting depths greater than 450 m were observed to feed primarily on euphausiids squid and rockfish, irrespective of size, likely due to prey availability as a function of depth and illustrating their generalist feeding behaviour (Robinson et al., 2007). While capture depths were not available for our samples, historical trawling locations and species composition for Central California (Miller et al., 2014) suggests that these samples were captured at depths less than 200 m. Longnose skate do not undergo an ontogenetic shift in depth distribution. Overall, longnose skate are classified as upper trophic level predators, albeit below apex predators such as Carcharhiniformes or Lamniformes sharks (Ebert and Bizzarro, 2007). Based on trophic level, it would seem reasonable to expect a phase lag of 1–2 years in the longnose skate pulse curve (i.e. shifted to the right of the petrale sole curve); however, we did not observe one. The longnose skate pulse curves, based on AFSC age estimates, were in fact shifted 1–3 years to the left of the petrale sole reference curve

Table 3
Non-linear mixed effects $\Delta^{14}C$ model parameters (median, lower 5%, higher 95%) from 2000 Markov Chain Monte Carlo (MCMC) simulations of the converged posterior sample for longnose skate age estimates for unstained samples. The first subscript of the random effects parameter identifies age reader (1,2 = AFSC; 3,4 = DFO, R = petrale sole (*Eopsetta jordani*, reference curve) and the second identifies the fixed effect to which the random effect parameter is associated. Also given are MCMC convergence statistics.

Parameter	Median	Lower	Higher	First order correlation	Geweke statistic, *z*	Pr > |*z*|
Fixed effects						
θ_2	155.25	148.16	162.63	0.042	0.174	0.861
θ_3	1963.07	1956.40	1969.50	0.028	0.104	0.916
θ_4	5.88	4.37	7.39	0.035	-0.043	0.965
Random effects						
u_{13}	1964.2	1957.9	1971.0	0.055	-0.895	0.371
u_{23}	1964.4	1957.7	1971.3	0.047	-0.175	0.860
u_{33}	1960.2	1953.3	1966.6	0.031	-1.054	0.292
u_{43}	1959.7	1952.9	1966.0	0.039	0.345	0.560
u_{R3}	1966.7	1960.5	1973.6	0.029	0.981	0.870
u_{14}	5.9	7.1	7.1	0.145	-0.561	0.982
u_{24}	5.9	4.7	7.2	0.005	0.879	0.563
u_{34}	4.7	3.5	5.9	0.028	-0.274	0.273
u_{44}	4.7	3.5	5.9	0.012	-0.173	0.764
u_{R4}	5.8	4.4	7.1	0.035	0.274	0.354
σ^2_e	599.4	531.1	693.4	0.019	1.583	0.123
$\sigma^2_{\theta 3}$	19.2	2.0	65.4	0.005	-0.051	0.959
$\sigma^2_{\theta 4}$	1.7	0.2	2.5	0.007	-0.121	0.798

(Table 3 and Fig. 6).

We cannot rule out that the asynchrony in radiocarbon pulse curves in our study might be influenced by our lack of specimens to fill in the pre-bomb (< 1959) and pre-midrise portions of the curve (< 1962) where $\Delta^{14}C$ data can be most informative (Helser et al., 2014). As such, to fit the model to the data we assumed that the lower asymptotes of the longnose skate $\Delta^{14}C$ curves were the same as those for the petrale sole reference observations; an assumption we could not verify due to lacking pre-bomb data. However, the analysis of Helser et al. (2014) who conducted a meta-analysis of $\Delta^{14}C$ data from 13 species in the North Pacific Ocean found the lower asymptote parameter (pre-bomb to initial rise) to be the least variable and the observed median value was close to that used in this study. Also, the longnose skate $\Delta^{14}C$ observations between 1965 and 1980 showed more variability than might be expected which may suggest the possibility that other process factors (other than ageing error) may affect the assimilation rates in a dissimilar manner than petrale sole. We assume that longnose skate used in this study experience the same environmental or oceanographic conditions, which mediate the available ^{14}C concentrations, and hence assimilation into the tissue, as the petrale sole reference. Helser et al. (2014) and Kastelle et al. (2015) among others have shown that oceanographic factors such as upwelling can complicate comparisons to reference chronologies when samples are collected from different regions. In fact the petrale sole reference curve itself was observed to have a phase lag in the radiocarbon rise compared to Pacific halibut (*Hippoglossus stenolepis*) captured throughout the Gulf of Alaska (Haltuch et al., 2013; Piner and Wischniowski, 2004). Since the petrale sole samples used were from their first year only, the phase lag was attributable to the upwelling of radiocarbon-depleted deep water into shallow regions (18–90 m) where juvenile petrale sole spend a substantial portion of time (Haltuch et al., 2013). As noted above, the longnose skate samples were likely captured at depths less than 200 m, and ontogenetic shifts in longnose skate depth distribution has not been noted. Without recorded depths for either species, we cannot attribute the phase lag that we observed to differences in depth distribution. However, given that upwelling is a local event with extreme variability by location, we cannot rule out that the phase lag reflects variability in deep-water, radiocarbon-poor, upwelling conditions experienced by the two species.

A further implicit assumption of this age validation method is that there are no biological differences between the validation species and reference chronology species in the deposition of ^{14}C in the structures being analyzed. This includes the above discussions on the sources of ^{14}C, either DIC or diet, and any metabolic reworking of the vertebrae. A further consideration is any metabolic or physiological differences between ^{14}C deposition in teleost otoliths and that deposited in elasmobranch vertebrae (Kalish, 1995). The best case exists when the validation and reference chronology samples are conspecific (Piner and Wischniowski, 2004). We assumed that petrale sole from the California Current would be an appropriate reference for longnose skate from the same region, but more work is needed to evaluate potential biological differences in ^{14}C uptake rates between the two species. This study is the first bomb radiocarbon age validation study of North Pacific skates, and demonstrates that more research is needed to help understand the sources of bomb radiocarbon in skate vertebrae.

Notwithstanding these issues, the Bayesian model results indicate that AFSC skate age estimation based on unstained thin sectioned vertebrae, while not completely free of ageing bias, are the least biased of the primary agencies responsible for ageing longnose skate along the North Pacific coast. This is a highly important result because minor refinements of the Gburski et al. (2007) age determination criteria may result in more accurate estimates and better consistency among ageing experts of the different Pacific coast agencies. Longnose skate age estimates which on average are possibly overaged by only 1–3 years is a tractable and manageable starting point to provide better life history parameter estimates for use in stock assessments. The results presented here suggest that the observed maximum age of 25 years for longnose skate and the corresponding estimated natural mortality rate (Hoenig and Gruber, 1983) of 0.17 reported in Gburski et al. (2007) for the Gulf of Alaska are reasonable since those ages were produced with the validated criteria presented here. Longnose skate specimens from other regions will need to be re-assessed with this validated age determination method to generate regional-specific growth curve parameter estimates and investigate any ecosystem effects on size-at-age and other life history parameters.

Non-linear mixed effect models, as was developed to analyze the data in this study, are particularly suited for clustered data in that they treat the nested nature of the data simultaneously and accounts for their overall mean structure as well as their variability both within and between subjects. Mixed effects models provide an advantage of "borrowing strength" from more robust data sets to improve parameter estimation of the weaker data set (Hilborn and Liermann, 1998; Myers and Mertz, 1998). This was certainly the case where pre mid-rise (< 1962) petrale sole $\Delta^{14}C$ observations informed the parameter estimation of the longnose skate pulse function where data were lacking or highly variable. This compromise has been described as

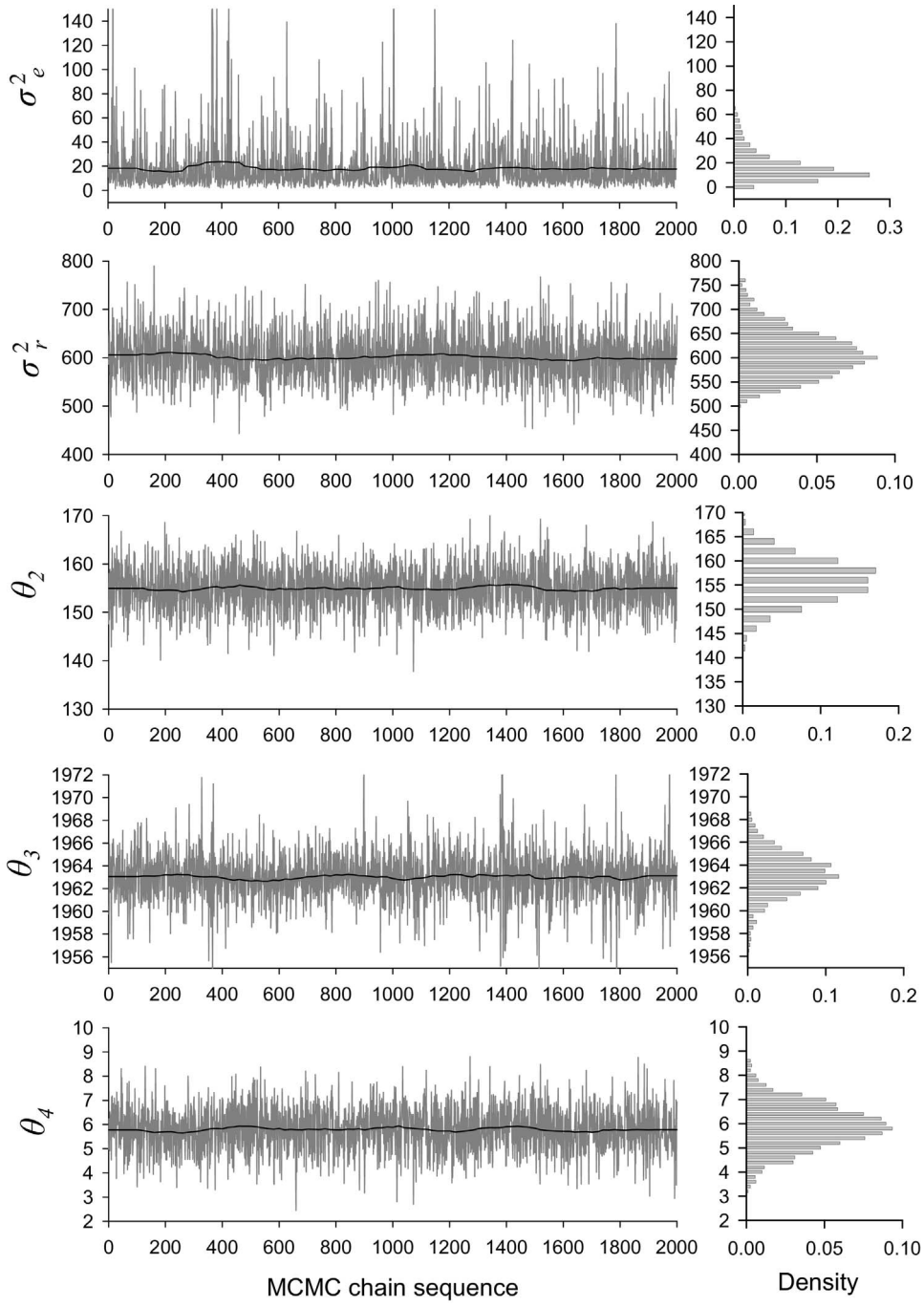

Fig. 5. Left panels: Markov Chain Monte Carlo (MCMC) traces for the five estimated parameters in the 4PL model describing radiocarbon incorporation in longnose skate vertebrae (Table 3). Gray lines show the 2000 samples for each parameter, solid lines show the cumulative median (up to that sample). Right panels: Marginal posterior distributions for each estimated model parameter.

"shrinkage" where parameters shrink toward the group mean when data are lacking or are uninformative (Gelman et al., 2004). In our case, the compromise enabled comparison of the petrale sole pulse function with and without the inclusion of longnose skate data. The longnose skate data had little influence on the estimated pulse curve from the more robust petrale sole data; conversely the petrale sole data were essential to estimate the longnose skate pulse curves. Inclusion of both longnose skate and petrale sole reference $\Delta^{14}C$ data and age reader as a random effect in the same non-linear model is not only desirable but quite justified. In this regard, the explicit assumption of the statistical model is equivalent to the implicit assumptions in bomb radiocarbon studies: that the validation and reference data are subject to the same environmental and biological processes affecting the uptake of ^{14}C. Application of this non-linear mixed effect model using MCMC simulation provides the added advantage in that hypothesis regarding ageing bias can easily be quantitatively tested and evaluated in a probabilistic framework.

Acknowledgments

Sandra Zeiner and Patricia Wolf collected the longnose skate and big skate vertebrae in 1980–1981. Romney McPhie assisted in vertebrae sectioning and micro-milling. Vanessa Hodes, Fisheries and Oceans Canada, and Beth Matta, National Marine Fisheries Service, were secondary readers in the interagency exchange portion of this project. Beth Matta provided comments and feedback on an earlier version

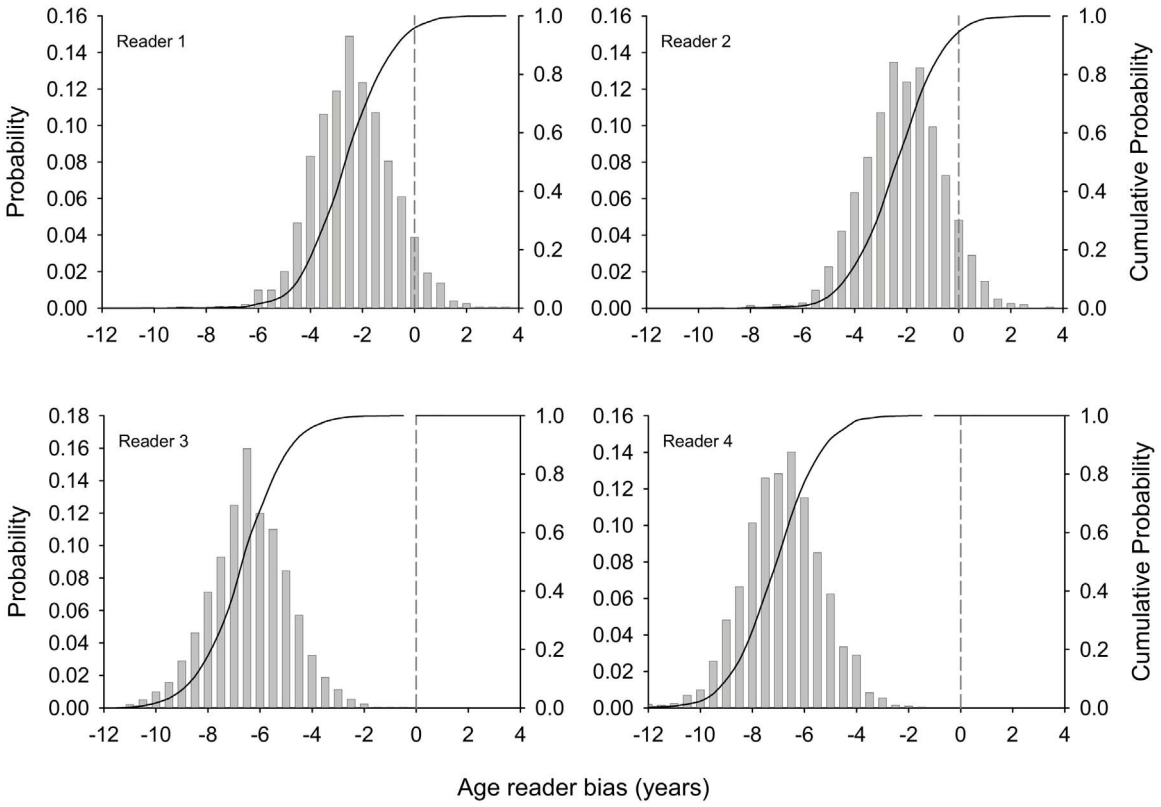

Fig. 6. Frequency histogram of 2000 MCMC outcomes for longnose skate defining bias, and the cumulative probability of bias > age$_x$ for unstained samples. The curve is a probability profile showing the probability of bias ($\Delta(\theta_{i3} - \theta_{R3})$) greater than a discrete number of years. Readers 1 and 2 are from AFSC; readers 3 and 4 are from DFO. Negative values indicate age over estimation.

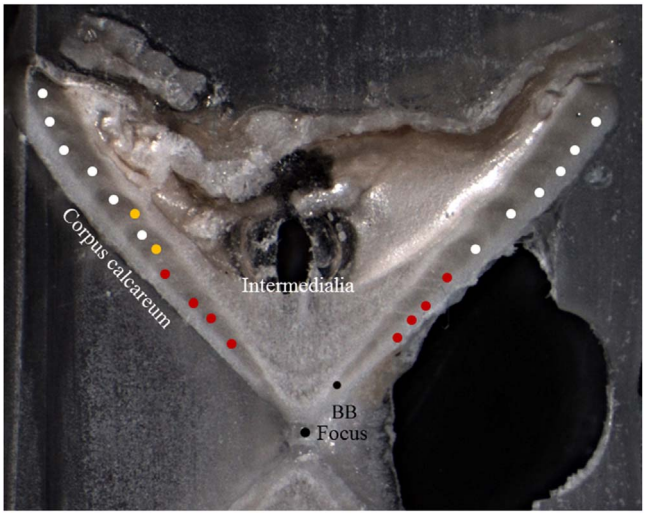

Fig. 7. Photo of longnose skate (sample RR30) vertebral thin section (unstained preparation method) under reflected light. Opaque bands appear white and translucent bands appear black. Annual band pairs are comprised of one opaque band and one translucent band. BB denotes 'birth band' which is formed when the skate hatches, and is not included in annual counts. The red dots denote the first four annual band pairs, which can be followed faintly across the intermedialia from one corpus calcareum to the other. Along the left corpus calcareum, 8 band pairs are noted by the white and yellow dots combined. However, the band pairs denoted by yellow dots are not observed on the right corpus calcareum, and therefore are not band pairs included in the annual count. The best age estimate for this sample, based on ageing criteria presented in this study, is 10 years. (For interpretation of the references to colour in this figure legend, the reader is referred to the web version of this article.)

which improved the manuscript. This work was supported by the North Pacific Research Board (Project 1202, NPRB publication number 637). The findings and conclusions in this paper are those of the authors and do not necessarily represent the views of the National Marine Fisheries Service.

References

Andrews, A.H., Kerr, L.A., 2015. Validated age estimates for large white sharks of the northeastern Pacific Ocean: altered perceptions of vertebral growth shed light on complicated bomb $\Delta^{14}C$ results. Environ. Biol. Fish. 98, 971–978.

Ardizonne, D., Cailliet, G.M., Natanson, L.J., Andrews, A.H., Kerr, L.A., Brown, T.A., 2006. Application of bomb radiocarbon chronologies to shortfin mako (*Isurus oxyrinchus*) age validation. Environ. Biol. Fish. 77, 355–366.

Beamish, R.J., Fournier, D.A., 1981. A method for comparing the precision of a set of age determinations. Can. J. Fish. Aquat. Sci. 38 (8), 982–983.

Cailliet, G.M., Goldman, K.J., 2004. Age determination and validation in chondrichthyan fishes. In: Carrier, J.C., Musick, J.A., Heithaus, M.R. (Eds.), Biology of Sharks and Their Relatives. CRC Press LLC, Boca Raton, FL, pp. 399–447.

Campana, S.E., Annand, M.C., McMillan, J.I., 1995. Graphical methods for determining the consistency of age determinations. Trans. Am. Fish. Soc. 124, 131–138.

Campana, S.E., Natanson, L.J., Myklevoll, S., 2002. Bomb dating and age determination of large pelagic sharks. Can. J. Fish. Aquat. Sci. 59, 450–455.

Campana, S.E., 2001. Accuracy, precision and quality control in age determination, including a review of the use and abuse of age validation methods. J. Fish. Bio. 59 (2), 197–242.

Chang, W.Y.B., 1982. A statistical method for evaluating the reproducibility of age determination. Can. J. Fish. Aquat. Sci. 39, 1208–1210.

Druffel, E.M., Linick, T.W., 1978. Radiocarbon in annual coral rings of Florida. Geophys. Res. Lett. 5, 913–916.

Dulvy, N.K., Metcalfe, J.D., Glanville, J., Pawson, M.G., Reynolds, J.D., 2000. Fishery stability, local extinctions, and shifts in community structure in skates. Conserv. Biol. 14 (1), 283–293.

Ebert, D.A., Bizzarro, J.J., 2007. Standardized diet compositions and trophic levels of skates (Chondrichthyes: rajiformes: Rajoidei). Environ. Biol. Fish. 80, 221–237.

Fry, B., 1988. Food web structure on Georges Bank from stable C, N, and S isotopic compositions. Limnol. Oceanogr. 33 (5), 1182–1190.

Gburski, C., Gaichas, S.K., Kimura, D.K., 2007. Age and growth of big skate (*Raja binoculata*) and longnose skate (*R. rhina*) in the Gulf of Alaska. Environ. Biol. Fish. 80, 337–349.

Gelman, A., Carlin, J.B., Stern, H.S., Rubin, D.B., 2004. Bayesian Analysis, 2nd ed. Chapman and Hall, New York, NY.

Gertseva, V.V., 2009. The population dynamics of the longnose skate, *Raja rhina*, in the northeast Pacific Ocean. Fish. Res. 95, 146–153.

Goldman, K.J., 2004. Age and growth of elasmobranch fishes. In: Musick, J.A., Bonfil, R. (Eds.), Technical Manual for the Management of Elasmobranchs. Asia Pacific Economic Cooperation and IUCN Shark Specialist Group Publication, pp. 97–132.
Haas, D., 2010. Skates and rays. In: Larinto, T. (Ed.), Status of the Fisheries Report ? An Update Through. CA Dept. of Fish and Game, pp. 1–17. Available at. http://www.dfg.ca.gov/marine/status/report2008/skates.pdf.
Haltuch, M.A., Hamel, O.S., Piner, K.R., McDonald, P., Kastelle, C.R., Field, J.C., 2013. A California Current bomb radiocarbon reference chronology and petrale sole (*Eopsetta jordani*) age validation. Can. J. Fish. Aquat. Sci. 70 (1), 22–31.
Hamel, O.S., Piner, K.R., Wallace, J.R., 2008. A robust deterministic model describing the bomb radiocarbon signal for use in fish age determination. Trans. Am. Fish. Soc. 137, 852–859.
Helser, T.E., Kastelle, C.R., Lai, H.-L., 2014. Modeling environmental factors affecting assimilation of bomb-produced $\Delta^{14}C$ in the North Pacific Ocean: implications for age validation studies. Ecol. Modell. 277, 108–118.
Hilborn, R., Liermann, M., 1998. Standing on the shoulders of giants: learning from experience in fisheries. Rev. Fish Biol. Fish. 8, 273–283.
Hoenig, J.M., Gruber, S.H., 1983. Empirical use of longevity data to estimate mortality rates. Fish. Bull. US 82, 898–902.
Kalish, J.M., Johnston, J., 1995. Determination of school shark age based on analysis of radiocarbon in vertebral collagen. In: Use of the Bomb Radiocarbon Chronometer to Validate Fish Age. Final Report. FDRC Project 93/109. Kalish J.M.. Fisheries Research and Development Corporation, Canberra, Australia, pp. 116–122.
Kalish, J.M., 1993. Pre- and post-bomb radiocarbon in fish otoliths. Earth Planet Sci. Lett. 114, 549–554.
Kalish, J.M., 1995. Radiocarbon and fish biology. In: Secor, D.H., Dean, J.M., Campana, S.E. (Eds.), Recent Developments in Fish Otolith Research. University of South Carolina Press, Columbia, SC, pp. 637–653.
Kastelle, C.R., Helser, T.E., Wischniowski, S.G., Lohr, T., 2015. Incorporation of bomb-produced ^{14}C into fish otoliths: a novel approach for evaluating age validation and bias with an application to yellowfin sole and northern rockfish. Ecol. Modell. 320, 79–91.
Kerr, L.A., Andrews, A.H., Cailliet, G.M., Brown, T.A., Coale, K.H., 2006. Investigations of $\Delta^{14}C$, $\delta^{13}C$ and $\delta^{15}N$ in vertebrae of white shark (*Carcharodon carcharias*) from the eastern North Pacific Ocean. Environ. Biol. Fish. 77, 337–353.
Lunn, D.J., Thomas, A., Best, N., Spiegelhalter, D., 2000. WinBUGS − a bayesian modelling framework: concepts, structure, and extensibility. Stat. Comput. 10 (4), 325–337.
McBride, R.S., 2015. Age and growth of big skate (Raja binoculata) and longnose skate (Raja rhina) in British Columbia waters. Fish. Res. 78, 2149–2167.
McFarlane, G.A., King, J.R., 2006. Age and growth of big skate (Raja binoculata) and longnose skate (Raja rhina) in British Columbia waters. Fish. Res. 78, 169–178.
McPhie, R.P., Campana, S.E., 2009. Bomb dating and age determination of skates (family Rajidae) off the eastern coast of Canada. ICES J. Mar. Sci. 66, 546–560.
Myers, R.A., Mertz, G., 1998. Reducing uncertainty in the biological basis of fisheries management by meta-analysis of data from many populations; a synthesis. Fish. Res. 37, 51–60.
Natanson, L.J., Sulikowski, J.A., Kneebone, J.R., Tsang, P.A., 2007. Age and growth estimates for the smooth skate, *Malacoraja senta*, in the Gulf of Maine. Environ. Biol. Fish. 80, 293–308.
Ormseth, O.A., Matta, B., 2009. Gulf of Alaska skates. Stock Assessment and Fishery Evaluation Report for the Groundfish Resources of the Gulf of Alaska Region. North Pacific Fishery Management Council, 605 W. 4th Ave., Suite 306 Anchorage, AK, pp. 99501.
Passerotti, M.S., Carlson, J.K., Piercy, A.N., Campana, S.E., 2010. Age validation of great hammerhead shark (*Sphyrna mokarran*), determined by bomb radiocarbon analysis. Fish. Bull. 108, 346–351.
Passerotti, M.S., Andrews, A.H., Carlson, J.K., Wintner, S.P., Goldman, K.J., Natanson, L.J., 2014. Maximum age and missing time in the vertebrae of sand tiger shark (*Carcharias taurus*): validated lifespan from bomb radiocarbon dating in the western North Atlantic and southwestern Indian Oceans. Mar. Freshwater Res. 65, 674–687.
Piner, K.R., Wischniowski, S.G., 2004. Pacific halibut chronology of bomb radiocarbon in otoliths from 1944 to 1981 and a validation of ageing methods. J. Fish. Biol. 65 (4), 1060–1071.
Pinheiro, J.C., Bates, D.M., 2000. Mixed-effects Models in S and S-PLUS. Springer Science and Business Media.
Robinson, H.J., Cailliet, G.M., Ebert, D.A., 2007. Food habits of the longnose skate, *Raja rhina* (Jordan and Gilbert 1880), in central California waters. Environ. Biol. Fish. 80, 165–179.
Smith, A., Wakefield, J., 1994. The hierarchical bayesian-Approach to population pharmacokinetic modeling. Int. J. Biomed Comput 36 (1-2), 35–42.
Spiegelhalter, D., Thomas, A, Best, N., Lunn, D., 2003. WinBUGS User Manual, Version 1.4 [online]. Available from http://www.mrc-bsu.cam.ac.uk/bugs (Accessed 22 April 2013).
Stuvier, M., Polach, H.A., 1977. Reporting of C-14 data. Radiocarbon 19, 355–363.
Thompson, J.E., 2006. Age, Growth and Maturity of the Longnose Skate (Raja Rhina) for the US West Coast and Sensitivity to Fishing Impacts MS Thesis. State University, Oregon.
Von Rosen, D., 1997. On moments of the inverted Wishart distribution. Statistics 30, 259–278.
Zeiner, S.J., Wolf, P.G., 1993. Growth characteristics and estimates of age at maturity of two species of skates (Raja binoculata and Raja rhina) from Monterey Bay, California. In: Branstetter, S. (Ed.), Conservation Biology of Elasmobranchs. US. Dept. Comm., NOAA Technical Report, NMFS 115, pp. 87–99.